

A Wavelet Based Synchronized Waveform Measurement Unit Algorithm

Kevin Kawal, Qiteng Hong, Panagiotis N. Papadopoulos
 Department of Electronic and Electrical Engineering
 University of Strathclyde
 Glasgow, UK
q.hong@strath.ac.uk

Steven M. Blair
 Synaptec
 Glasgow, UK
steven.blair@synaptc.ec

Campbell D. Booth
 Department of Electronic and Electrical Engineering
 University of Strathclyde,
 Synaptec
 Glasgow, UK
campbell.d.booth@strath.ac.uk

Abstract—Power systems with high penetrations of inverter-based resources are increasingly vulnerable to severe disturbances which may manifest as non-stationary voltage and current waveforms, presenting challenges to phasor measurement units which assume quasi-stationary conditions. Time synchronized, high-resolution, waveform measurements have emerged as a solution to accurately monitor emerging system dynamics. This paper proposes a synchronized waveform measurement unit algorithm to detect and characterize transient and dynamic phenomena present in synchronized waveform measurements. The proposed method utilizes the discrete wavelet packet transform to represent non-sinusoidal transients, while the adaptive empirical wavelet transform is applied to extract the fundamental and possible oscillation components. Finally, dynamic phasor extraction is performed via the Hilbert transform. The performance of the proposed algorithm is evaluated using synthetic test signals and compared to a phasor measurement unit algorithm using a goodness of fit metric. The results indicate that the proposed method produces an accurate and sparse representation of the underlying signal dynamics. The proposed method can potentially reduce communication requirements associated with high resolution synchronized waveform measurements, thus enabling real-time synchronized waveform-based applications.

Keywords—synchronized waveforms, power system transients, power system oscillations, phasor measurement unit, wavelet transform

I. INTRODUCTION

In response to continued efforts towards achieving net-zero carbon emissions targets, the generation profile of power systems is evolving to include increasing volumes of power electronic inverter-based resources (IBRs, e.g. wind, PV, HVDC systems, etc.) to replace fossil fuel-driven synchronous generators (SGs). The displacement of SGs by IBRs has led to an overall decrease in system inertia and strength, increasing system volatility following disturbances and threatening the stability of the network [1]. In the context of IBR-dominated networks, there is an increased risk of extreme transient and dynamic behaviour propagating throughout the network leading to cascading failures and potential blackouts [1]. Several real-world disturbances have been observed recently including unintentional IBR tripping due to phase jumps [2] and IBR driven sub-synchronous oscillations (SSO) [3]. Accurate monitoring, detection and characterization of power system transients and dynamics are therefore critical to enable appropriate and timely mitigation of such events, thus ensuring the continued adoption of IBRs while meeting environmental and operational constraints.

Phasor measurement units (PMUs) have been increasingly adopted in power networks, enabling time synchronized

voltage and current phasors (synchrophasors) across large geographical areas of the network. PMUs employ signal processing techniques that assume quasi-stationary (near constant frequency during time interval of interest) and steady-state (nominal frequency) sinusoidal conditions [4]. PMUs therefore extract and characterize a single fundamental component that is assumed to be stationary throughout the observation window. However, power system transients and emerging IBR driven dynamics result in conditions that violate the assumptions made in traditional phasor estimation techniques.

Fig. 1(a) illustrates a digital fault recorder (DFR) current waveform during a cable fault reported in [5]. Sub-cycle transients result in a broad frequency spectrum with energy distributed in higher frequency ranges (relative to the nominal frequency, i.e. 50 Hz) as illustrated in Fig. 1(b). Power system transients (e.g. faults, lightning surges, switching events) that have broadband frequency spectra cannot be represented by traditionally defined narrowband (fundamental) phasors [6]. Fig. 1(c) illustrates the voltage waveform for a simulated IBR driven SSO, representative of a real-world scenario as presented in [3]. The amplitude envelope is shown to highlight the distortions present in the waveform. The frequency spectrum of this waveform shown in Fig. 1(d) shows non-fundamental components manifesting as side-band inter-harmonic oscillations centered around the fundamental frequency. PMU measurements have been subject to aliasing under such conditions [3]. PMUs, therefore, while still critical to power system monitoring, will face severe limitations in system disturbances, which increase in occurrence and severity in IBR dominated power networks.

In this context, high resolution (1-61kHz), time-synchronized (to universal coordinated time (UTC)) voltage

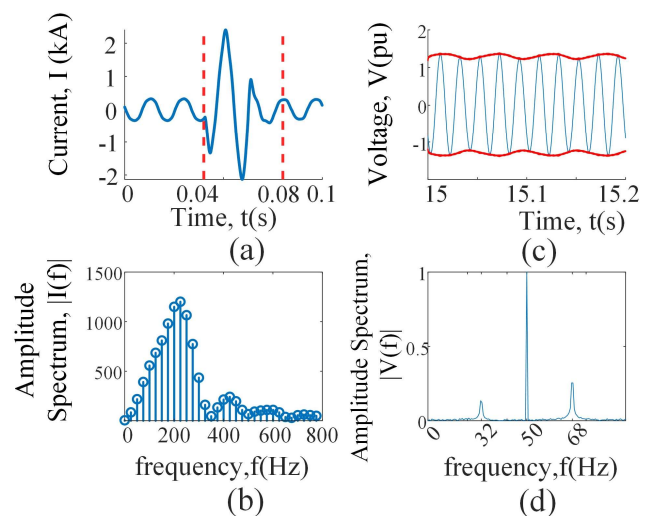


Fig 1. Frequency domain characteristics of power system disturbances.

This research is funded by CENSIS, Synaptec, UK and by project RESCUE (EP/T021829/1). P. N. Papadopoulos is supported by a UKRI Future Leaders Fellowship [MR/S034420/1]. All results can be fully reproduced using the methods and data described in this paper and references provided.

and current waveform measurements (sync-waves) have emerged as a potential solution [7]. Such measurements may be produced by DFRs, power quality (PQ) meters (with additional time synchronization) and more recently distributed sensing platforms [8] and can accurately capture power system dynamics. However, high bandwidth communication requirements, data storage and computational burden associated with processing high resolution measurements are key challenges to real-time utilization of sync-waves, particularly at a wide-area scale [9]. Predetermined, trigger-based processing may also fail to account for emerging IBR driven dynamics [7]. Improved signal processing techniques are required to detect and accurately characterize disturbances measured by sync-waves, which PMUs cannot capture, thus improving situational awareness and facilitating the mitigation of such disturbances.

In [10], a real-time sub-synchronous phasor measurement algorithm is presented. The fundamental component is filtered out and modal filtration combined with a recursive discrete Fourier transform (DFT) is used to extract sub-synchronous components. This results in voltage and current phasors at sub-synchronous frequencies of interest. Such a technique is application specific and does not capture the fundamental component. A wavelet based phasor estimation algorithm is presented in [11] to detect fundamental and harmonic/inter-harmonic phasors. [10] and [11] present enhanced PMU methods in the presence of non-stationary conditions but cannot represent transients. The work reported in [12] extracts Lissajous curves from voltage and current sync-waves and uses similarity metrics to compare Lissajous curves obtained under steady-state and disturbance conditions. Results indicate that the extracted features can be used to detect, localize, and classify events. In [13], short time Fourier transform (STFT) is applied to voltage and current waveforms to produce time-frequency spectrums of different PQ events. These are then input into machine learning (ML) based classifiers, which are used to differentiate and classify different events. Such methods as proposed in [12] and [13] extract features of transients that are suitable for data-analytic processing, but do not report physically meaningful representations (amplitude, phase, frequency) of steady state or evolving power system dynamics.

Ref. [6] addresses the aforementioned limitations associated with application specific sync-wave processing by defining several functional bases representing steady state and power system dynamics, for example frequency ramps, amplitude modulations and phase jumps. Each functional basis is characterized by an expression described by relevant parameters. A dictionary of functional bases is predefined for expected parameter ranges. Optimization techniques are then employed to find the functional bases and parameters that optimally represent the signal. Such an approach expands on PMU techniques, which can be thought of as using a single fundamental frequency sinusoidal basis, by incorporating different possible transient and dynamic references. The dictionary design incorporates domain knowledge and provides a sparse representation (via a fixed set of parameters) of power system disturbances. However, the dictionary design is complex and it is difficult to pre-determine and accurately describe all possible disturbances via unique functional bases. Real-time optimization can also be computationally expensive.

This paper proposes a sync-wave measurement unit

algorithm that can extract features to accurately characterize abnormal power system signals and is adaptable to different system disturbances. Power system disturbances are broadly categorized as broad-spectrum transients and narrow spectrum oscillatory components. The proposed method performs a two-stage decomposition of the input signal. Firstly, the discrete wavelet packet transform (DWPT) is applied to detect and represent the broad-spectrum components as wavelet features relative to discrete higher-frequency sub-bands. Oscillatory components including the fundamental component are then processed using the frequency adaptive empirical wavelet transform (EWT), which allows for isolating of narrow spectrum frequency components. The Hilbert transform, (HT) is then applied to each detected component to extract time varying amplitude, phase, and frequency within the observation window. The outputs of the algorithm therefore include fundamental phasors and, where present, oscillation (harmonic/inter-harmonic) phasors at the detected frequency and a wavelet feature matrix of highly distorted components. The proposed method therefore measures steady state conditions and via the flexibility of the wavelet bases, adapts in real-time to different possible signal dynamics, including highly distorted waveforms.

The rest of the paper is structured as follows: Section II briefly introduces the theory of the DWPT and EWT transforms and describes the proposed algorithm; results using synthetic and real-world data representing different disturbances are presented and discussed in Section III; considerations of the algorithm performance are discussed in Section IV; and finally, conclusions and future work are highlighted in Section V.

II. PROPOSED METHOD

A. Discrete Wavelet Packet Transform

The discrete wavelet transform (DWT) analyses a signal using a set of functional bases, $\psi_{j,k}$, derived from scaling and translating a mother wavelet, $\psi(n)$ [14]:

$$\psi_{(j,k)}(n) = 2^{\frac{j}{2}} \times \psi(2^{-j}n - k), \quad (1)$$

where j represents the decomposition level and k influences the translation. The wavelets are scaled by 2^j and translated by $2^j k$ steps allowing for different discrete frequency and time supports respectively. The DWT is equivalent to bandpass filtering of the input signal at discrete frequency levels called scales. To ensure full coverage of the signal spectrum a scaling function, $\phi(n)$, which is equivalent to a low pass filter, is applied. The wavelet decomposition of a signal at the j^{th} scale can be implemented as an iterative filter operation with the high-pass and low pass filter designs based on the wavelet and scaling functions respectively. The DWT decomposes a signal into detail (high-frequency) and approximation (low-frequency) components. Subsequent approximation components are then similarly decomposed. The DWPT builds on the DWT by successively decomposing both the detail and approximation components at each decomposition level resulting in higher frequency resolution compared to the DWT. DWPT results in sub-band filtering of the input signal into 2^j equal sub-bands. The improved frequency resolution and time-frequency localization properties of the DWPT therefore makes it suitable for analyzing broad-spectrum transient signals. The Daubechies wavelet with 4 vanishing moments (db4), used in this paper, has good time localization properties and has been widely applied in analyzing power

system transients and power quality phenomena [15]. A fixed decomposition level of 5 was adopted in this paper resulting in 32 sub-bands to give improved frequency resolution in analyzing transient events.

B. Empirical Wavelet Transform

The EWT represents an adaptive wavelet basis that is adaptable to the frequency content of the input signal [16]. The frequency spectrum of the input signal is obtained and an optimal segmentation of the frequency spectrum is performed. The segmentation, described by a set of boundary frequencies, Λ_n , is then used to define the wavelet and scaling functions and hence the frequency supports of the wavelets. Expressions for the EWT wavelet and scaling functions are derived and presented [16]. The EWT is equivalent to bandpass filtering on each detected frequency spectrum boundary as opposed to the fixed scale levels of the DWPT. The EWT can therefore decompose a multi-component signal into single frequency components. EWT implementation is dependent on the signal characteristics as well as the targeted application and is a trade-off between accurate signal representation and noise rejection. The level of segmentation which defines the signal decomposition level is attributed to determining the significant spectrum peaks. In this paper, peaks greater than 1% of the fundamental are retained. This is chosen to obtain early detection of dynamics including harmonics or sideband (sub/super- synchronous oscillation components) IBR-driven oscillations. Spectrum segmentation is achieved via spectrum peak location and determining distances between adjacent frequency peaks or finding the nearest (local) minima from each peak.

C. Synchronized Waveform Measurement Unit Algorithm

The proposed algorithm is illustrated in Fig. 2. A two stage DWPT-EWT signal decomposition is applied to sync-wave samples. Note that the front-end signal processing and time synchronization of the raw data is not described in this paper. The DWPT detects and represents transients as a wavelet coefficient matrix representing the spread of energy in the frequency domain amongst higher frequency sub-bands. These broad-spectrum components are then filtered (zeroing of high frequency wavelet coefficients) to produce a signal with narrow band oscillatory components. The adaptability of the EWT is then utilized to detect and isolate the different frequency components including the fundamental and possible harmonic/inter-harmonic components. Removal of the broad-spectrum transient components has the additional benefit of increasing the performance of the frequency spectrum segmentation of the EWT and hence the ability to isolate the possible oscillatory components present in the signal. The output of the EWT is a decomposition of the signal into intrinsic mode functions (IMFs) that contain a single dominant frequency.

A phasor extraction method is then applied to extract synchrophasors defined at the specific IMF frequency. A synchrophasor per IMF is therefore generated. In this paper the Hilbert Transform (HT) is applied for phasor extraction. The HT, $\tilde{x}(t)$, of a real signal, $x(t)$, is given by:

$$\tilde{x}(t) = \frac{1}{\pi} \int_{-\infty}^{\infty} \frac{x(\tau)}{t-\tau} d(\tau). \quad (2)$$

This represents a 90-degree rotation of the signal.

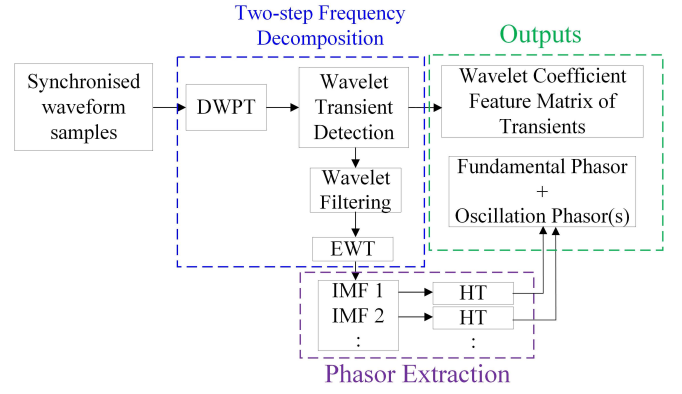


Fig 2. Proposed SWMU algorithm

The combination of the real signal and its HT gives the complex valued analytical signal as

$$\hat{x}(t) = x(t) + j\tilde{x}(t). \quad (3)$$

The analytic signal can be used to obtain the instantaneous phase angle of the signal as

$$\tan^{-1} \left(\frac{\tilde{x}(t)}{x(t)} \right). \quad (4)$$

The instantaneous frequency of the signal can then be extracted as the angular velocity of the analytic signal. The magnitude of the analytic signal corresponds to the amplitude envelope of the real valued input signal. HT based phasor methods therefore present a framework to represent power system dynamics as dynamic phasors [17].

The proposed method therefore seeks to achieve enhanced performance over conventional PMUs, which use a single reference basis that assumes quasi-stationary conditions. The Daubechies wavelet bases provides a representation of the severely distorted, transient conditions, that cannot be represented by traditional phasors, via a time-frequency wavelet-based feature matrix. The adaptable EWT and HT based phasor estimation tracks multiple components at frequencies on interest (e.g. for, fundamental, harmonics, IBR driven SSO frequencies).

III. RESULTS

The proposed algorithm was implemented in the MATLAB/Simulink environment using the MATLAB wavelet toolbox [18] and the EWT function based on [16]. The algorithm was tested on a wide range of signals as presented in the following subsections.

A. Synthetic Data

A synthetic test signal, v , comprising of a phase jump described by (5) and harmonics, described by (6), is used to evaluate the performance of the proposed algorithm.

$$v = X_{rms}(\sqrt{2})\cos\left(2\pi f_o t + k_a u(t_{ph})\right), \quad (5)$$

$$v = X_{rms}(\sqrt{2})\cos(2\pi f_o t) + \sum_n X_{n,rms}(\sqrt{2})\cos(2\pi n f_o t), \quad (6)$$

where, X_{rms} , is set as 1V, f_o , is set as 50Hz, k_a , represents the step change in angle and is set as 45 degrees, $u(t_{ph})$, is a unit step function at time, t_{ph} , set as 0.32s in this example. Harmonics are introduced at 0.56s and n specifies the harmonic order with second and fourth harmonic used in this paper. $X_{2,rms}$, is set as 0.15V and $X_{4,rms}$, is set as 0.1V.

The test signal is input to the proposed algorithm. The DWPT outputs a wavelet matrix, $|V(t,f)|$ consisting of a wavelet decomposition of the high-frequency sub-bands associated with the broad-spectrum transient. This can be visualized as the wavelet energy spectrum as illustrated in Fig. 3. This result demonstrates that the proposed algorithm can localize the phase angle jump while extracting relevant features that describe the underlying dynamics associated with the transient condition. The signal is then filtered by thresholding the high frequency sub-band wavelet coefficients. This is then input to the EWT module which decomposes the signal into the fundamental and harmonic components. The HT then extracts the amplitude, phase, and frequency of each detected component. Fig. 4 illustrates the Hilbert spectrum of the algorithm output. It is observed that the fundamental frequency and harmonic components are accurately measured.

B. Comparison with PMU

To assess the performance of the proposed method in comparison to a traditional PMU algorithm, the test signal was processed by an M class compliant PMU algorithm described in [19]. Typically, PMUs are assessed using total vector error (TVE). This metric assesses how accurately the PMU measures the assumed stationary signal. However, it does not give any insights into the ability of the phasor output to accurately represent the actual signal characteristics which may contain non-stationary disturbances. To measure this, a goodness of fit (GoF) metric described in [20] is adopted in this paper as the basis for comparing the performance of the proposed method and PMUs. GoF is defined as follows:

$$GoF = 20 \log \frac{X_m}{\sqrt{\frac{1}{(N-m)} \sum_{k=1}^N (u_k - v_k)^2}}, \quad (7)$$

where X_m is the signal amplitude, N is the number of samples, m is the number of parameters being estimated, u_k is the signal value, v_k is the estimated sample. A large GoF indicates that the measurement and signal are a good match. Experiments with physical PMUs and real-world data has shown that values greater than 40dB represent a good fit [20]. The outputs of the proposed algorithm and PMU are used to reconstruct the input signal as illustrated in Fig. 5(a). Note that the transient component is reconstructed via an inverse DWPT and added to the fundamental and harmonic phasor reconstruction. Fig 5(b) clearly demonstrates that the proposed algorithm produces a higher GoF during the phase jump and the time in which the harmonics are present. The advantage of dynamic phasor estimation via the HT, over traditional PMU measurements, in tracking step changes within the observation window is also demonstrated via the relatively shorter time in which the GoF metric increases after the onset of the event.

C. Simulated and Real-world data

IBR driven oscillations can manifest as inter-harmonic oscillations with multiple components. The frequencies of these oscillations are determined by grid strength, operating conditions and proprietary IBR controllers making it difficult to predict the frequency range of potential oscillations. A test system representative of an IBR connected to a weak grid described in [3] was simulated in the Real-Time Digital Simulator. The simulated data, illustrated in Fig. 1(c), was input into the proposed algorithm. The Hilbert spectrum of the algorithm output is illustrated in Fig 6(a). The distorted waveform contains sideband oscillations at approximately 68

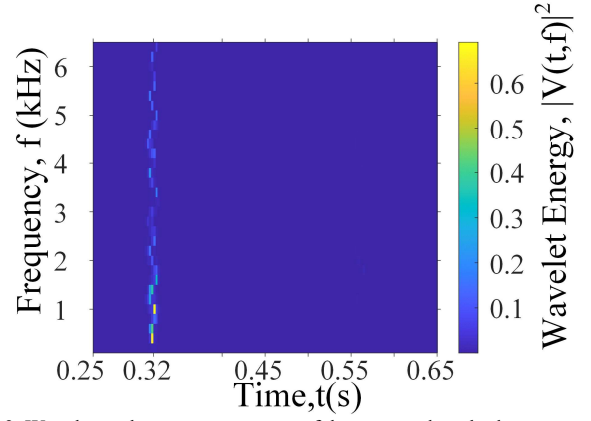


Fig 3. Wavelet packet spectrum output of the proposed method.

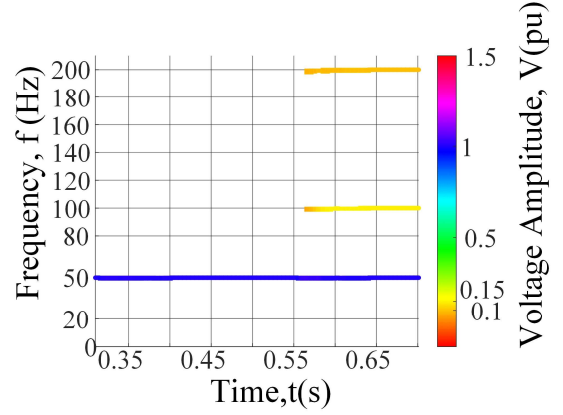


Fig 4. Hilbert spectrum output of the proposed method

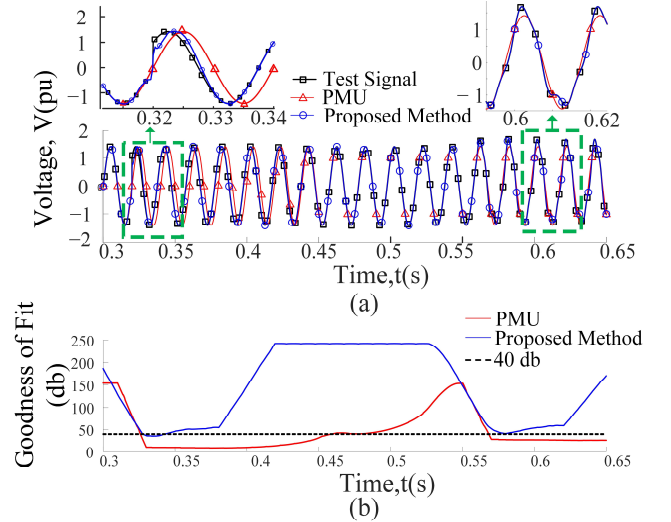


Fig 5. Comparison of the proposed method and M class PMU, (a) waveform reconstruction, (b) goodness of fit analysis

and 32 Hz which are successfully detected and tracked by the proposed algorithm. This demonstrates that adaptability of the EWT to the frequency spectrum of the input signal is beneficial for IBR-driven SSO monitoring applications. Real-world waveform data, attributed to a damaged cable available in [5] and illustrated in Fig 1(a), was input to the proposed algorithm. Fig. 6(b) illustrates the wavelet packet spectrum output obtained. This shows that the proposed algorithm can extract time-frequency (wavelet domain) features of distorted real-world measurements. Comparing with Fig. 3, the frequency content of different transient conditions present different wavelet spectrums. Such features can therefore be used in classifying different transient events.

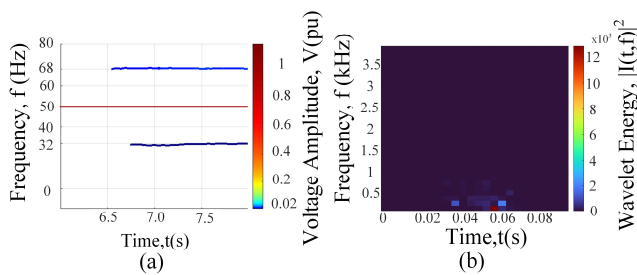


Fig 6. (a) Hilbert spectrum of simulated IBR driven SSO, (b) Wavelet packet energy spectrum of real-world power system transient.

IV. DISCUSSION

The test results presented in Section III demonstrate the suitability of the proposed algorithm in accurately representing the underlying dynamics that may be present in sync-wave measurements. During steady state the proposed algorithm will simply output a fundamental phasor. In the presence of harmonics/inter-harmonics, phasors at the detected frequency will be output. Under sub-cycle or highly distorted conditions a wavelet feature matrix provides a time-frequency representation of the signal. The proposed algorithm is adaptable to a wide range of transient/dynamic conditions and provides a sparse representation (compared to the raw waveform) of the dynamics present in sync-wave measurements. This can eliminate the need for constant transmission of high volumes of data, reducing real time communication requirements, and thus enabling real time wide area sync-wave based applications. The accurate measurement of transients can enable wavelet-based protection schemes, while sparse representation of signal dynamics can enable applications such as IBR driven oscillation monitoring. The outputs can also be used to reconstruct the original signal more accurately via the inverse DWPT and phasor reconstruction, thus reducing storage requirements and allowing for further insights to be gained, for example feature extraction for training machine learning applications. The proposed method uses a fixed level of decomposition for the DWPT while the impacts of noise were also not addressed. However optimal decomposition and wavelet based de-noising methods using an appropriate cost function can be incorporated. The design is therefore a trade-off between accuracy, noise rejection and computational burden.

V. CONCLUSION AND FUTURE WORK

This paper has presented an SWMU algorithm that is adaptable to different transient and dynamic phenomena that may be increasingly present in IBR dense power networks. DWPT is applied to represent non-sinusoidal transients, while the adaptive EWT decomposes the input signal into fundamental and oscillation components. Finally, the HT is applied to extract dynamic phasors at the detected frequencies. The proposed algorithm was tested using a synthetic dataset and benchmarked against a PMU algorithm. The results indicate that the proposed algorithm provides a significantly more accurate measurement of the underlying dynamics present in the input signal. Finally, features extracted from datasets representing real-world disturbances highlight the potential applications of the proposed algorithm. Future work involves investigation of bandwidth requirements for real time streaming of SWMU outputs, assessment of the latency of proposed algorithm and further refinement and optimization for real-time hardware implementation.

REFERENCES

- [1] A. Tuohy, P. Dattaray, E. Farantatos, A. Kelly and E. Lannoye, "Implications of reduced inertia levels on the electricity system: Technical Report on the challenges and solutions for system operators with very high penetrations of non-synchronous resources," EPRI, Palo Alto, CA, USA, 3002014970, Jun. 2019.
- [2] North American Electric Reliability Corporation, "1,200 MW Fault Induced Solar Photovoltaic Resource Interruption Disturbance Report," Atlanta, GA, USA, Jun. 2017.
- [3] L. Fan et al., "Real-World 20-Hz IBR Subsynchronous Oscillations: Signatures and Mechanism Analysis," *IEEE Transactions on Energy Conversion*, vol. 37, no. 4, pp. 2863–2873, Dec. 2022, doi: 10.1109/TEC.2022.3206795.
- [4] *IEEE/IEC International Standard - Measuring relays and protection equipment - Part 118-1: Synchrophasor for power systems - Measurements*, IEC/IEEE 60255-118-1:2018 Std., Dec. 2018.
- [5] *DOE/EPRI Disturbance Library*, Electric Power Research Institute, May, 2023. [Online]. Available: <https://pqdl.epri.com>.
- [6] A. Karpilow, A. Derviskadic, G. Frigo, and M. Paolone, "Characterization of Non-Stationary Signals in Electric Grids: A Functional Dictionary Approach," *IEEE Trans. Power Syst.*, vol. 37, no. 2, pp. 1126–1138, Mar. 2022, doi: 10.1109/TPWRS.2021.3105295.
- [7] W. Xu, Z. Huang, X. Xie, and C. Li, "Synchronized Waveforms – A Frontier of Data-Based Power System and Apparatus Monitoring, Protection, and Control," *IEEE Trans. Power Delivery*, vol. 37, no. 1, pp. 3–17, Feb. 2022, doi: 10.1109/TPWRD.2021.3072889.
- [8] P. Orr et al., "Distributed Photonic Instrumentation for Power System Protection and Control," *IEEE Transactions on Instrumentation and Measurement*, vol. 64, no. 1, pp. 19–26, Jan. 2015, doi: 10.1109/TIM.2014.2329740.
- [9] J. Follum et al., "Phasors or waveforms: considerations for choosing measurements to match your application," Pacific Northwest National Laboratory, PNNL-31215, Apr. 2021.
- [10] X. Xie, W. Liu, H. Liu, Y. Du, and Y. Li, "A System-Wide Protection Against Unstable SSCI in Series-Compensated Wind Power Systems," *IEEE Transactions on Power Delivery*, vol. 33, no. 6, pp. 3095–3104, Dec. 2018, doi: 10.1109/TPWRD.2018.2829846.
- [11] K. Chauhan, M. V. Reddy, and R. Sodhi, "A Novel Distribution-Level Phasor Estimation Algorithm Using Empirical Wavelet Transform," *IEEE Trans. Ind. Electron.*, vol. 65, no. 10, pp. 7984–7995, Oct. 2018, doi: 10.1109/TIE.2018.2801837.
- [12] M. Izadi and H. Mohsenian-Rad, "Characterizing Synchronized Lissajous Curves to Scrutinize Power Distribution Synchro-Waveform Measurements," *IEEE Trans. Power Syst.*, vol. 36, no. 5, pp. 4880–4883, Sep. 2021, doi: 10.1109/TPWRS.2021.3084447.
- [13] C. Sticht, "Power System Waveform Classification Using Time-Frequency and CNN," ORNL/SPR-2021/2381, 1841478, Jan. 2022, doi: 10.2172/1841478.
- [14] M. Stéphane, "CHAPTER 7 - Wavelet Bases," in *A Wavelet Tour of Signal Processing* (Third Edition), M. Stéphane, Ed., Boston: Academic Press, 2009, pp. 263–376. doi: 10.1016/B978-0-12-374370-1.00011-2.
- [15] S. Avdaković and N. Čišija, "Wavelets as a tool for power system dynamic events analysis – State-of-the-art and future applications," *Journal of Electrical Systems and Information Technology*, vol. 2, no. 1, pp. 47–57, May 2015, doi: 10.1016/j.jesit.2015.03.005.
- [16] J. Gilles, "Empirical Wavelet Transform," *IEEE Transactions on Signal Processing*, vol. 61, no. 16, pp. 3999–4010, Aug. 2013, doi: 10.1109/TSP.2013.2265222.
- [17] A. Derviskadic, G. Frigo, and M. Paolone, "Beyond Phasors: Modeling of Power System Signals Using the Hilbert Transform," *IEEE Trans. Power Syst.*, vol. 35, no. 4, pp. 2971–2980, Jul. 2020, doi: 10.1109/TPWRS.2019.2958487.
- [18] The MathWorks, Inc. (2022). *Wavelet Toolbox (R2022b)*. Accessed: May 02, 2023. Available: <https://www.mathworks.com>.
- [19] A. J. Roscoe, I. F. Abdulhadi, and G. M. Burt, "P and M Class Phasor Measurement Unit Algorithms Using Adaptive Cascaded Filters," *IEEE Transactions on Power Delivery*, vol. 28, no. 3, pp. 1447–1459, Jul. 2013, doi: 10.1109/TPWRD.2013.2238256.
- [20] A. Riepnick and H. Kirkham, "An Introduction to Goodness of Fit for PMU Parameter Estimation," *IEEE Transactions on Power Delivery*, vol. 32, no. 5, pp. 2238–2245, Oct. 2017, doi: 10.1109/TPWRD.2016.2616761.